Strain effect on thermal conductivity of 3C-SiC nanowire ⊘

Wenkang Chen (iD) ; Xiangshui Wu; Shichen Deng; Nuo Yang ✉ (iD) ; Xiangfan Xu ✉ (iD)

Check for updates

View Online   Export Citation

11 September 2024 08:16:00

AIP Publishing

Strain effect on thermal conductivity of 3C-SiC nanowire

View Online   Export Citation   CrossMark

Wenkang Chen,[1] (iD) Xiangshui Wu,[1] Shichen Deng,[2] Nuo Yang,[2,a] (iD) and Xiangfan Xu[1,a] (iD)

AFFILIATIONS

[1]Center for Phononics and Thermal Energy Science, China-EU Joint Center for Nanophononics, School of Physics Science and Engineering, Tongji University, Shanghai 200092, China
[2]Department of Physics, National University of Defense Technology, Changsha 410073, China

Note: This paper is part of the APL Special Collection on Advances in Thermal Phonon Engineering and Thermal Management.
[a]Authors to whom correspondence should be addressed: nuo@hust.edu.cn and xuxiangfan@tongji.edu.cn

ABSTRACT

Strain provides an additional mechanism in tuning the thermal/electrical properties of nanostructures and therefore has triggered lots of interest in recent years. However, experimental research about the strain effect on the thermal conductivity of nanowires is still limited, especially in the low-temperature range, which is important in understanding the physics of strain-induced regulation in thermal conductivity. Here, we present thermal transport measurements of bent silicon carbide nanowires at temperatures ranging from 20 to 300 K. Reduction in thermal conductivity compared to their straight counterparts is observed. More specifically, the relative change is up to 55% at 20 K and descends with temperature, which is due to the inhomogeneous strain-induced phonon scattering. This study will deepen the understanding of thermal properties in nanostructures with strain.

Low-dimensional materials have triggered tremendous interest for decades and have been vastly studied for their novel physical phenomena and potential applications in magnetic, electronic, and thermoelectric devices.[1–3] Investigating the thermal conductivity of low-dimensional materials is essential for addressing challenges in electronic devices, energy conversion, and thermal management.[4,5] The capability to tailor thermal properties at the nanoscale provides new possibilities for advancing technology and designing materials with specific thermal properties. Thermal properties of low-dimensional materials can be modulated through doping,[6] size/dimension effect,[7,8] strain effect,[9,10] etc., allowing for customization to meet the demand in various specific applications.

The strain effect is important in the thermal transport of nanostructured materials both from a fundamental and application point of view. Strain can cause atomic deformation in the nanostructure, which can change the lattice constant and tune phonon dispersion,[10–12] consequently affecting thermal conductivity by changing phonon group velocity, specific heat, and phonon scattering rate. From an application point of view, nanowires, such as silicon carbide (SiC) and silicon nanowires, usually serve as fillers to composites, for example, interfacial thermal materials, for enhancing their mechanical, electrical, and thermal performance,[13–15] and the mechanical bend or stress from

external force is a common issue in those composites in real application scenarios. In addition, it is difficult to ensure a strain-free environment for low-dimensional devices and they will commonly hold residual strain, either from the fabrication process or the local thermal expansion of the substrate.[16]

Therefore, the strain effect on the mechanical and thermal properties of nanowires has triggered great interest.[17–20] For instance, Li et al.[10] systematically studied the strain effects on the thermal conductivity of nanostructures, including silicon thin film and graphene flake, and found that thermal conductivity decreases continuously as the applied strain is changed from compressive to tensile, owing to the shift of phonon dispersions. In addition, phonon–phonon scattering can be directly affected by altering the anharmonicity of the lattice. For example, MD simulation on bent silicon nanowires[21] observed a reduction of up to 10% in thermal conductivity, which is attributed to the depression of long wavelength phonons and enhanced local phonon scattering.[22] Similar results can be found in the literatures where the physics behind the strain-induced regulation in thermal conductivity has triggered great interest.[23–27] To clarify whether phonon group velocity or phonon anharmonicity dominates the strain-induced thermal conductivity, the temperature dependence of strain effect needs to be carried out, which, however, is rare due to the difficulty of experiments.

In this manuscript, we implement thermal transport measurement on bent 3C-SiC nanowires (Shanghai Aladdin Biochemical Technology Co., Ltd., China) with temperatures ranging from 20 to 300 K. The reduction in thermal conductivity of bent nanowires is up to 55% at 20 K, compared to the straight counterparts. In addition, the relative change of thermal conductivity decreases with temperature and shows an increased trend with the applied strain.

We implement thermal properties characterization by the thermal bridge method (Fig. 1),[28–30] which has been developing as a mature method in micro-/nanoscale materials thermal transport measurement. Thermal contact resistance is an important issue of the thermal bridge method,[31] and one should clarify this before acquiring accurate experimental results. The measured thermal resistance R_s contains two parts, intrinsic thermal resistance R_i of SiC nanowires, and the two thermal contact resistance between SiC nanowires and the membranes R_c, i.e., $R_s = R_i + R_c$. Even though R_c cannot be directly measured, we can still extract it by fitting:

$$R_s \times d = \frac{4}{\pi \times \kappa} \times \frac{L}{d} + R_c \times d, \quad (1)$$
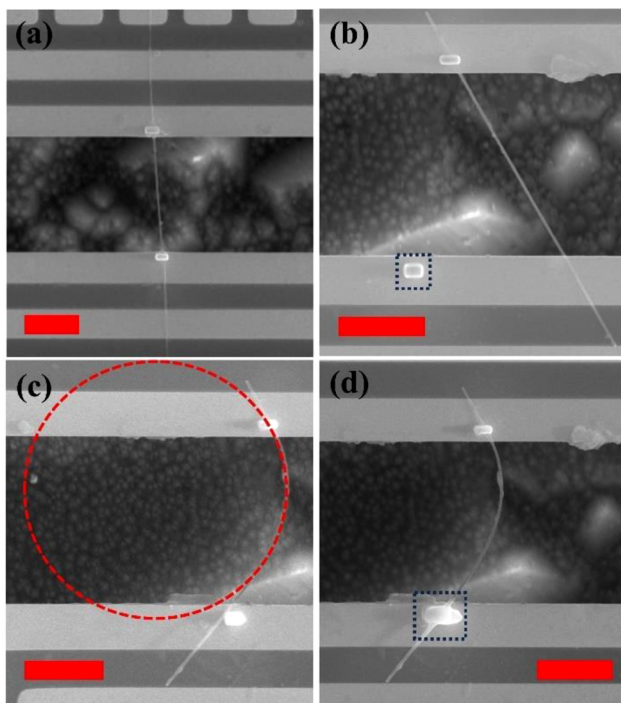

FIG. 1. SEM image of suspended SiC nanowires on the thermal bridge. A single homogeneous SiC nanowire was cut into two parts. (a) One part is transferred onto the thermal bridge for comparison with two ends fixed by the Pt/C pad. (b) The other is also transferred onto a thermal bridge for the preparation of bent SiC nanowires. One end of this nanowire is fixed by a Pt/C pad, and a Pt pillar is deposited in the opposite membrane (blue rectangle). (c) The free end of the SiC nanowire is bent by micro-manipulate and blocked by the Pt/C pillar. The red circle fits the curvature of the bent SiC nanowire, and its diameter is 16.9 μm. (d) The Pt/C pad is again deposited onto the end blocked by the Pt/C pillar as denoted by the blue rectangle, for fixing and improving the thermal contact. The scale bars here are 5 μm.

where L is the length of suspended nanowires, d is the diameter of the nanowire, and κ is the thermal conductivity. As shown in Fig. 2(a), linear fitting lines at 100, 180, and 300 K are demonstrated. The intercepts here are nearly zero, which indicates the thermal contact resistance is negligible in our measurement.

Overall, eight straight and three bent 3C-SiC nanowires with diameters ranging from 120 to 280 nm are studied. Figure 2(b) shows the temperature-dependent thermal conductivity of eight straight samples. They show a consistent thermal conductivity ($33 \pm 2\, \mathrm{Wm^{-1}\,K^{-1}}$) at ambient temperature, implying no evident diameter dependence. The thermal conductivity at room temperature of single crystal 3C-SiC was measured to be $330\, \mathrm{Wm^{-1}\,K^{-1}}$,[32] while studies about SiC nanowires give a range of $12\text{–}120\, \mathrm{Wm^{-1}\,K^{-1}}$ due to differences in crystallinity and geometric size.[33–35] Therefore, the thermal conductivity of 3C-SiC nanowires measured here is reasonable. According to the XRD results (Fig. S1), the average grain size (40 ± 9 nm) here is much smaller than the diameter of 3C-SiC nanowires, which renders the grain boundary scattering the main reason for this relatively low thermal conductivity.

To study the bent/strain effect of thermal conductivity, single and long nanowires are used to exclude any measurement error from thermal contact, as well as the possible inherent strain difference from samples with different diameters. First, a long and uniform nanowire is cut into two nanowires by the micro-manipulator (Imina Technologies Micromanipulation Platform). One serves as the straight nanowire for comparison and is transferred to a thermal bridge by the micro-manipulator and thermally bridges two suspended membranes [Fig. 1(a)]. Then, Pt/C pads are deposited, through the gas injection system (GIS), to fix two ends of nanowires, which can induce additional thermal path to improve the thermal contact between the nanowire and membranes/electrodes.[36] The other is also transferred onto a thermal bridge, but only one end is fixed onto the membrane by Pt/C deposition, while a Pt/C pillar is deposited in the other membrane [blue dotted rectangle in Fig. 1(b)]. The free end of the SiC nanowire is then bent with the micro-manipulator and blocked by the Pt pillar from relaxation [Fig. 1(c)]. Finally, the Pt/C pad is deposited again to fix this end [Fig. 1(d)], which helps enhance the thermal contact and ensures it is consistent with the straight one.

To calculate the strain in bent SiC nanowires, we refer to the loop test method and define the stress and strain as:[37]

$$\varepsilon_{\max} = E \times \sigma_{\max} = E \times \frac{d}{D}, \quad (2)$$

where E is Young's modulus[38] and d and D are the diameter of the nanowire and the diameter of the nanowire loop, respectively. Notably, the strain of bent nanowires is inhomogeneous along the radial direction of the nanowire, in which compression strain and tensile strain coexist, and $\varepsilon_{\max}$ and $\sigma_{\max}$ represent the maximum stress and strain of the bent nanowire. Equation (2) indicates that strain changes linearly from positive to negative when stress changes from compression to tensile.

Three sets of samples with different strains, 1.93%, 1.51%, and 1.02%, are measured. Taking Young's modulus of the [111]-oriented SiC nanowires to be 500 GPa,[38] their stress is calculated to be 5.09, 7.25, and 9.66 GPa, respectively. Notably, it is just an estimation because [111] is not the only crystallographic orientation [Fig. S1(a)]. The details of these samples are listed in Table I.
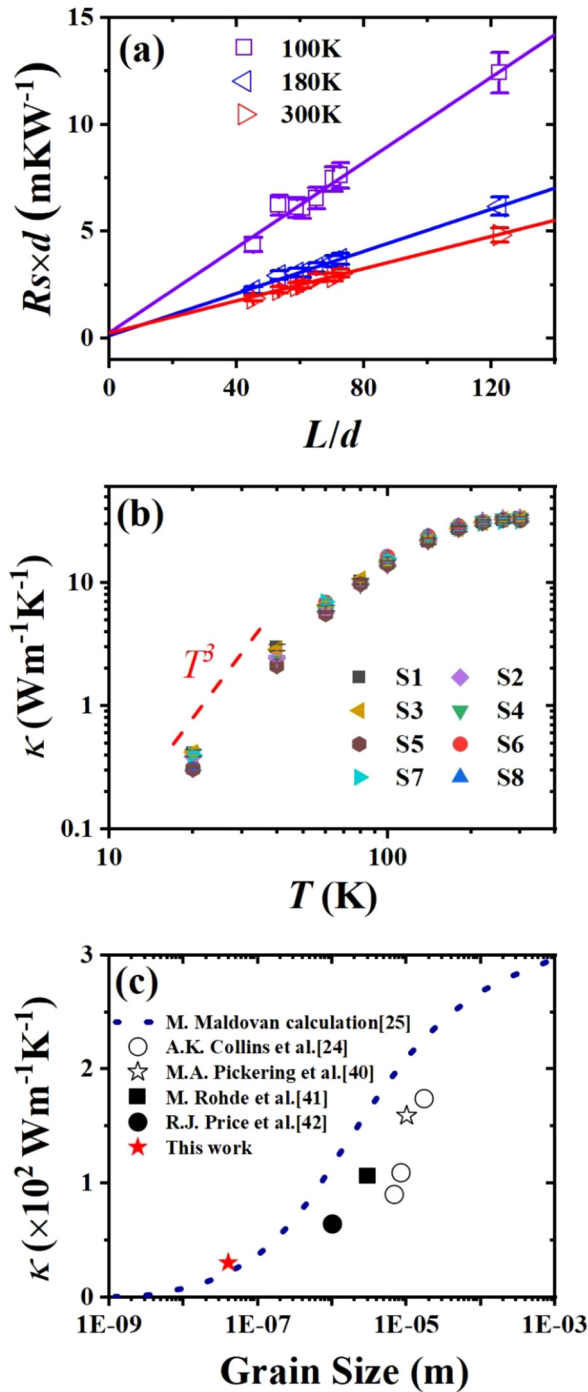
FIG. 2. (a) The fitting lines of $R_s \times d$ vs L/d at 100, 180, and 300 K show the intercept of nearly zero, indicating negligible thermal contact resistance. (b) The diameter-independent thermal conductivity of straight 3C-SiC nanowires with temperature ranging from 20 to 300 K. (c) The predicted relationship between room temperature thermal conductivity and grain size in 3C-SiC[26] (blue dashed line), along with previous experimental data by Collins *et al.*,[49] Pickering *et al.*,[50] Rohde,[51] and Price.[52] The thermal conductivity in this work is consistent with the theoretical prediction (red pentagram).

TABLE I. The details of bent 3C-SiC nanowires.

No.	d (nm)	D (μm)	σ_{max} (%)	η (20 K) (%)
B1	170	16.9	1.02	28
B2	145	9.6	1.51	36
B3	200	10.4	1.93	55

The thermal conductivity of one bent sample vs temperature is demonstrated in Fig. 3(a), which is remarkably suppressed compared with the corresponding straight nanowires. For clarity, here we define the relative change of thermal conductivity as

$$\eta = \frac{\kappa_i - \kappa_b}{\kappa_i} \times 100\%, \qquad (3)$$

where κ_i and κ_b are the thermal conductivity of intrinsic/straight nanowire and bent nanowire. A negative correlation is reflected between η and temperature, reaching up to 55% at 20 K for the nanowire with 1.93% strain, and being less than 10% when $T > 100$ K.
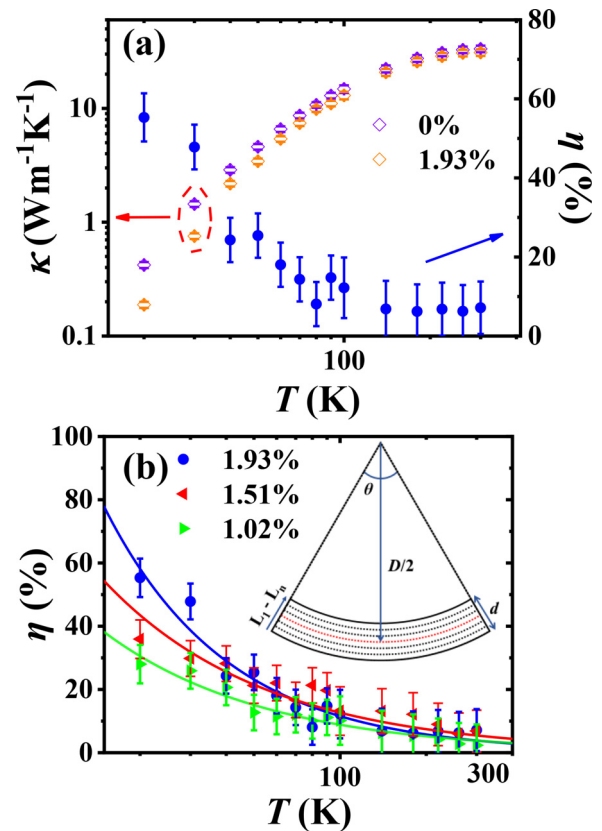
FIG. 3. (a) Comparison of thermal conductivity between straight and bent 3C-SiC nanowires. (b) The relative change of thermal conductivity η reaches up to 55% at $T = 20$ K in a bent nanowire of 1.93% strain and decreases with temperature. At low temperatures, η shows an evident increasing trend with strain. Inset shows the schematic diagram of a bent SiC nanowire divided into many layers; d is the diameter of the nanowire, while D is the diameter of the fitting circle.

11 September 2024 08:16:00

All bent 3C-SiC nanowires show a descending η with temperature [Fig. 3(a)].

Notably, the strain in the bent nanowires is nonuniform. The normal stress is compressive on the concave side while tensile on the convex side. It is known that the compressive strain will reduce the lattice constant, which will modify phonon dispersion and change the group velocity and specific heat.[10] Compressive strain can cause an increase in thermal conductivity, while tensile strain has the opposite effect, i.e., thermal conductivity decreases continuously as the applied strain is changed from compressive to tensile. It seems that these two kinds of strains should be symmetrically distributed and will counteract each other, which is, however, different from our measurement results here that thermal conductivity decreases with increasing strain.

Few mechanisms have been proposed to explain the strain-introduced thermal conductivity variation in nanowires. One of the mechanisms is related to the diffusive-ballistic mixture picture. A notable effect from the strain can be found when the radius of the curvature is one order of magnitude smaller than the phonon mean free path. It is proposed that the curvature impedes ballistic phonon transport in nanowires by phonon-boundary scattering and therefore reduces the thermal conductivity.[23,25,39] This effect can be enhanced with a lower temperature where the phonon mean free path is longer, which seems quite satisfactory to our results. However, as mentioned above, these nanowires measured are polycrystals with grain sizes of about 40 nm [Fig. S1(a)], which suggests that the phonon mean free path should be much less than the radius of the curvature, meaning the diffusive-ballistic picture is illogic here.

To further uncover the physics mechanism of the strain effect, the thermal conductivity $\kappa \sim cvl$ under the phonon gas model will be discussed, where c, v, and l are, respectively, the specific heat (has limited strain effect), the phonon group velocity, and the phonon mean free path. Both phonon group velocity and the phonon mean free path/relaxation time are believed to change under strain, but their contributions to thermal conductivity are material-dependent. For example, Li *et al.* found that mode-specific group velocities of phonons decrease continuously from compressive to tensile,[10] while Tang *et al.* showed that both phonon relaxation time and group velocity shift dramatically.[40] Similar results can also be found in other studies.[24,41,42] To distinguish the different contributions from group velocity and phonon relaxation time, low-temperature thermal conductivity is studied. As shown in Fig. 3(b), η changes from ~10% (at room temperature) to ~55% (at low temperatures), with nearly five times of magnitude enhancement, strongly suggesting that the thermal conductivity change under strain in this study is due to phonon relaxation time since acoustic phonon group velocity is believed to be near temperature independent.[43] This scenario is consistent with the inset of Fig. 3(b) that thermal conductivity decreases due to the additional phonon scattering from inhomogeneous strain along the nanowire radius.

As shown in the inset of Fig. 3(b), the bent nanowire can be divided into many layers along the radial direction, i.e., L_1 to L_N for analysis.[21] The strain can be assumed to be uniform in each layer, and it changes from compress strain to tensile strain along the radial direction. Thus, every layer will have different phonon dispersion, which means the overall phonon dispersion will broaden. This is confirmed by the very recent research on bent silicon nanoribbons.[44] This phonon dispersion broadening would increase the phonon frequencies for available scatterings and therefore promote and accelerate the phonon–phonon scattering rate. In addition, as nanowires are bended, the phonon incident angle changes when across different layers, modifying the scattering matrix and shortening the phonon lifetime.[45,46]

The temperature-dependent strain effect on thermal conductivity can now be understood by the following picture. At higher temperatures, the magnitude of η decreases with temperature and the increasing trend with strain is not obvious due to the experimental errors, while in the low-temperature range, thermal transport in stress-free nanowires is dominated by long-wavelength phonons, which are mainly scattered by the grain boundary. In bent nanowires, phonon scattering is enhanced due to strain-induced defects and variation in the scattering matrix, leading to an evident reduction in thermal conductivity. However, in the high-temperature range, the Umklapp process dominates thermal transport over the strain effect. The mean free path of phonons is remarkably suppressed, rendering the strain effect trivial. Consequently, a reduction in thermal conductivity is more evident in the low-temperature range than that in the high-temperature range.

Finally, we discuss the possible strain/curvature changes with decreasing temperature due to the possibly different thermal expansion coefficients between micro-bridges and the samples. The thermal expansion coefficient of polycrystal 3C-SiC[47] is found to be around $2.8 \times 10^{-6} \, \mathrm{K}^{-1}$, while that of thin film SiN_x[48] is about $3.3 \times 10^{-6} \, \mathrm{K}^{-1}$. These low thermal expansion coefficients and small differences between the two materials indicate that the length/curvature changes should be less than 0.1% as temperature descends, leading to negligible stress effect from curvature when temperature changes, according to Eq. (2).

In summary, we measured the thermal conductivity of eight straight and three bent SiC nanowires by the thermal bridge method. A reduction in bent SiC nanowires is observed compared to straight samples. Additionally, relative thermal conductivity change shows a decreasing trend with increasing temperature and an increasing trend with the applied strain at low temperatures. Our results suggest that phonon scattering from the inhomogeneous deformation by strain along the radial direction of the nanowire is the key to the reduction of thermal conductivity.

See the supplementary material for details of SiC nanowires characterization including x-ray diffraction and Raman spectrum (Fig. S1), and the analysis of experimental errors.

AUTHOR DECLARATIONS
Conflict of Interest

The authors have no conflicts to disclose.

Author Contributions

Wenkang Chen: Data curation (equal); Formal analysis (equal); Methodology (equal); Writing – original draft (equal). **Xiangshui Wu:** Data curation (equal); Formal analysis (equal); Investigation (equal); Writing – original draft (equal). **Shichen Deng:** Data curation (equal); Investigation (equal). **Nuo Yang:** Formal analysis (equal);

Writing – review & editing (equal). **Xiangfan Xu:** Conceptualization (equal); Funding acquisition (equal); Project administration (equal); Resources (equal); Supervision (equal); Validation (equal); Writing – review & editing (equal).

DATA AVAILABILITY

The data that support the findings of this study are available from the corresponding authors upon reasonable request.

REFERENCES

[1]A. A. Balandin, Nat. Mater. **10**(8), 569 (2011).

[2]M. F. L. De Volder, S. H. Tawfick, R. H. Baughman, and A. J. Hart, Science **339**(6119), 535 (2013).

[3]S. Manzeli, D. Ovchinnikov, D. Pasquier, O. V. Yazyev, and A. Kis, Nat. Rev. Mater. **2**(8), 17033 (2017).

[4]D. G. Cahill, W. K. Ford, K. E. Goodson, G. D. Mahan, A. Majumdar, H. J. Maris, R. Merlin, and S. R. Phillpot, J. Appl. Phys. **93**(2), 793 (2003).

[5]D. G. Cahill, P. V. Braun, G. Chen, D. R. Clarke, S. Fan, K. E. Goodson, P. Keblinski, W. P. King, G. D. Mahan, A. Majumdar, H. J. Maris, S. R. Phillpot, E. Pop, and L. Shi, Appl. Phys. Rev. **1**(1), 011305 (2014).

[6]T. Xing, C. X. Zhu, Q. F. Song, H. Huang, J. Xiao, D. D. Ren, M. J. Shi, P. F. Qiu, X. Shi, F. F. Xu, and L. D. Chen, Adv. Mater. **33**(17), 2008773 (2021).

[7]X. Wu, Q. Tao, D. Li, Q. Wang, X. Zhang, H. Jin, J. Li, S. Wang, and X. Xu, Nano Res. **14**(12), 4725 (2021).

[8]J. Guo, Y. Huang, X. Wu, Q. Wang, X. Zhou, X. Xu, and B. Li, Phys. Status Solidi RRL **13**(3), 1800529 (2019).

[9]F. Ma, H. B. Zheng, Y. J. Sun, D. Yang, K. W. Xu, and P. K. Chu, Appl. Phys. Lett. **101**(11), 111904 (2012).

[10]X. Li, K. Maute, M. L. Dunn, and R. Yang, Phys. Rev. B **81**(24), 245318 (2010).

[11]J. F. Meng, N. V. Chandra Shekar, J. V. Badding, D.-Y. Chung, and M. G. Kanatzidis, J. Appl. Phys. **90**(6), 2836 (2001).

[12]D. A. Polvani, J. F. Meng, N. V. Chandra Shekar, J. Sharp, and J. V. Badding, Chem. Mater. **13**(6), 2068 (2001).

[13]F. He, Y. Liu, Z. Tian, C. Zhang, F. Ye, L. Cheng, and L. Zhang, Mater. Sci. Eng., A **734**, 374 (2018).

[14]T. Han, R. Luo, G. Cui, and L. Wang, J. Eur. Ceram. Soc. **39**(5), 1743 (2019).

[15]B. M. Curtin, E. W. Fang, and J. E. Bowers, J. Electron. Mater. **41**(5), 887 (2012).

[16]C. Shao, X. Yu, N. Yang, Y. Yue, and H. Bao, Nanoscale Microscale Thermophys. Eng. **21**(4), 201 (2017).

[17]Y. Gao and Z. L. Wang, Nano Lett. **7**(8), 2499 (2007).

[18]J. Chen, G. Conache, M.-E. Pistol, S. M. Gray, M. T. Borgström, H. Xu, H. Q. Xu, L. Samuelson, and U. Håkanson, Nano Lett. **10**(4), 1280 (2010).

[19]X. Han, L. Kou, X. Lang, J. Xia, N. Wang, R. Qin, J. Lu, J. Xu, Z. Liao, X. Zhang, X. Shan, X. Song, J. Gao, W. Guo, and D. Yu, Adv. Mater. **21**(48), 4937 (2009).

[20]D. Rossouw and G. A. Botton, Phys. Rev. Lett. **110**(6), 066801 (2013).

[21]X. Liu, H. Zhou, G. Zhang, and Y.-W. Zhang, J. Appl. Phys. **125**(8), 082505 (2018).

[22]J. Huang, Y. Zhang, A. Fan, Y. Li, H. Wang, W. Ma, and X. Zhang, ACS Appl. Mater. Interfaces **15**(33), 39689 (2023).

[23]V. Lee, R. Chen, and C.-W. Chang, Phys. Rev. B **87**(3), 035406 (2013).

[24]S. Bhowmick and V. B. Shenoy, J. Chem. Phys. **125**(16), 164513 (2006).

[25]L.-C. Liu, M.-J. Huang, R. Yang, M.-S. Jeng, and C.-C. Yang, J. Appl. Phys. **105**(10), 104313 (2009).

[26]M. Maldovan, J. Appl. Phys. **110**(11), 114310 (2011).

[27]S.-D. Guo, J. Dong, and J.-T. Liu, Phys. Chem. Chem. Phys. **20**(34), 22038 (2018).

[28]L. Shi, D. Li, C. Yu, W. Jang, D. Kim, Z. Yao, P. Kim, and A. Majumdar, J. Heat Transfer **125**(5), 881 (2003).

[29]X. Xu, L. F. C. Pereira, Y. Wang, J. Wu, K. Zhang, X. Zhao, S. Bae, C. Tinh Bui, R. Xie, J. T. L. Thong, B. H. Hong, K. P. Loh, D. Donadio, B. Li, and B. Özyilmaz, Nat. Commun. **5**(1), 3689 (2014).

[30]L. Dong, B. Liu, Y. Wang, and X. Xu, Chin. Phys. Lett. **39**(12), 127201 (2022).

[31]J. Chen, X. Xu, J. Zhou, and B. Li, Rev. Mod. Phys. **94**(2), 025002 (2022).

[32]L. L. Snead, T. Nozawa, Y. Katoh, T.-S. Byun, S. Kondo, and D. A. Petti, J. Nucl. Mater. **371**(1), 329 (2007).

[33]L. A. Valentín, J. Betancourt, L. F. Fonseca, M. T. Pettes, L. Shi, M. Soszyński, and A. Huczko, J. Appl. Phys. **114**(18), 184301 (2013).

[34]K. Takahashi, Y. Ito, T. Ikuta, T. Nishiyama, M. Fujii, X. Zhang, and A. Huczko, High Temp. - High Pressures **37**(2), 119 (2008), available at https://search.ebscohost.com/login.aspx?direct=true&db=a9h&AN=34195141&site=ehost-live.

[35]K.-M. Lee, S.-K. Lee, and T.-Y. Choi, Appl. Phys. A **106**(4), 955 (2012).

[36]Q. Wang, Y. Chen, A. Aiyiti, M. Zheng, N. Li, and X. Xu, Chin. Phys. B **29**(8), 084402 (2020).

[37]S. Wang, Y. Wu, L. Lin, Y. He, and H. Huang, Small **11**(14), 1672 (2015).

[38]E. W. Wong, P. E. Sheehan, and C. M. Lieber, Science **277**(5334), 1971 (1997).

[39]J. Ma, Y. Ni, S. Volz, and T. Dumitrică, Phys. Rev. Appl. **3**(2), 024014 (2015).

[40]D.-S. Tang, G.-Z. Qin, M. Hu, and B.-Y. Cao, J. Appl. Phys. **127**(3), 035102 (2020).

[41]K. D. Parrish, A. Jain, J. M. Larkin, W. A. Saidi, and A. J. H. McGaughey, Phys. Rev. B **90**(23), 235201 (2014).

[42]Z. Huang, Z. Tang, J. Yu, and S. Bai, J. Appl. Phys. **109**(10), 104316 (2011).

[43]A. Mobaraki, C. Sevik, H. Yapicioglu, D. Çakır, and O. Gülseren, Phys. Rev. B **100**(3), 035402 (2019).

[44]L. Yang, S. Yue, Y. Tao, S. Qiao, H. Li, Z. Dai, B. Song, Y. Chen, J. Du, D. Li, and P. Gao, Nature **629**, 1021 (2024).

[45]Y. Ni, S. Xiong, S. Volz, and T. Dumitrică, Phys. Rev. Lett. **113**(12), 124301 (2014).

[46]K. Ohashi, J. Phys. Soc. Jpn. **24**(3), 437 (1968).

[47]G. A. Slack and S. F. Bartram, J. Appl. Phys. **46**(1), 89 (1975).

[48]C.-L. Tien and T.-W. Lin, Appl. Opt. **51**(30), 7229 (2012).

[49]A. K. Collins, M. A. Pickering, and R. L. Taylor, J. Appl. Phys. **68**(12), 6510 (1990).

[50]M. A. Pickering, R. L. Taylor, J. T. Keeley, and G. A. Graves, Nucl. Instrum. Methods Phys. Res., Sect. A **291**(1), 95 (1990).

[51]M. Rohde, J. Nucl. Mater. **182**, 87 (1991).

[52]R. J. Price, J. Nucl. Mater. **46**(3), 268 (1973).